Submission to

Journal of Magnetism and Magnetic Materials

Elsevier Editions

MS: MAGMA_2019_2241_R1

***

Magnetic properties dependence of mesoscopic scale thick films on thickness and surface roughness characteristics: Case of nickel samples in Ni/Pt system

by

Jean Ebothé *

Laboratoire de Recherche en Nanosciences (LRN), E.A. n° 4682, UFR Sciences Exactes, Université de Reims, 21 rue Clément Ader, 51685 Reims cedex 02, France

* *

(*) Corresponding author – Phone: (33) 3 26 05 19 01

Fax: (33) 3 26 05 19 00

E-mail: *jean.ebothe@univ-reims.fr*

Abstract

Thickness (d) and surface roughness (σ) of material thin films are inseparable characteristics engendered by the same deposition process. Both are crucial parameters for magnetic properties (p) of real mesoscopic scale thick ferromagnetic films. When condition $(d/\sigma) < 10^2$ *is validated, sorting out samples of a series is possible only by means of* $\tau = (d/\sigma)$ *geometrical ratio which enables their coherent comparison. Their magnetic properties (p) are thereby expressed in a single function form* $p=f(\tau)$*. Application of that approach to a series of nanostructured Ni electrodeposits reveals that these samples are consistent with the ratio range* $1.23 \leq \tau \leq 82.00$ *concurring with the reported description. Their coercivity (*H_c*) and magnetic domain size (w) behave in agreement with their respective predicted general curve profile when d is substituted by τ, which depicts quite well the similar role of both parameters. The study of these properties evolution using the normalization model indicates a discontinuity in the magnetism of the investigated samples. Bloch magnetic domains (*$MD)_B$ *are associated with mixed domain walls (*DW_N+DW_B*) below a critical position (*τ_0^{-1}*)* ≈ 0.35*, while Néel domain walls (*DW_N*) coexist with mixed magnetic domains (*MD_B+MD_N*) beyond that position.*

Keywords:

Mesoscopic scale thick films; surface topography; thin film's magnetic properties; magnetic microstructures

1. INTRODUCTION

The behaviour of ferromagnetic material thin films submitted under a magnetic field is basically assigned to their chemical composition and structure phase. However, the studies on their actual properties always represent a complicated task either in theory or experiment. Decreasing the sample size, as currently executed nowadays, enhances the difficulty of entirely matching the results obtained from both different approaches. Once surface adsorption phenomenon and probable internal impurities are controlled, the film global geometry can play a determining role on its behaviour. Thickness and surface topography together represent quite well that geometrical feature. Thickness is the most commonly investigated film characteristic which mainly reflects its core or bulk content configuration. In the frame of *nano* science and technology, thinner specimens can produce better feed-back usually explored in the fabrication of sensors and many other modern device systems [1–3]. Surface topography depicts the material interruption zone, bearing for that reason a typical microstructure and morphology which engenders some modifications under the magnetic field effect compared to bulk. Its impact on magnetic film's properties is nowadays widely evidenced [4–6]. By and large, the study of individual role of surface or bulk part on a film physical behaviour is undertaken by approximation, neglecting the little contribution of one of them [8–10]. This clearly indicates that their complete separation is impossible, regardless of experimental methods used for the samples deposition and characterization. We have to admit that such an approximation can never be systematic due to various situations linked to elaboration process of real material thin films. In actual fact, usual approximating procedures are very restrictive since one excludes the case of samples having equal impact of both film parts and also the situation when these procedures are impossible. In practice, the easier assumption is sometimes quickly adopted, stating for instance that surface topography aspects have a limited effect on the film behaviour. This explains the little attention paid so far to the mentioned *unusual* situations. The extensive solicitation of mesoscopic scale thick samples including nano-films and nano-structured specimens in the building of modern device systems prompts to carefully examine all other possible options keeping in mind that surface morphology and bulk interconnect closely as both of them result from the same film growth process. Consequently, only a clear and rational approach to their mutual relationship with film properties can emerge onto consistent interpretations. Theoretical studies on these properties evolution are tremendously improved when they remain as close as possible to a detailed description of the film behaviour, even though that description derive from simple

models. As a matter of fact, simplifications or approximations are always associated with strict conditions to be fulfilled in any theory application. Accordingly, reduction of simplifications in analytical treatments makes the theory potentially in better agreement with the film material reality. The calculated property is thereby more adapted to the actual behaviour of the investigated sample.

In the present proposal, the study is focused on the evolution of nano-structured film's magnetic properties, insisting on the particular case for which approximation or simplification in the relationship between bulk and surface contributions is impossible. This is a "*non trivial*" situation practically ignored in the literature of material thin films. An original approach to that evolution is proposed. Sections 2 and 3 are devoted to a concrete study of Ni films formed using a specific electro-deposition protocol. Application of that approach to these film's magnetic properties is reported, followed by identification of the sample's magnetic microstructures evolved that contribute to their ferromagnetism manifestation.

2. EXPERIMENTAL DETAILS

The Ni samples investigated are prepared by cathodic voltammetry (C-V) technique described previously [7] using a three-electrode cell system consisted of 1 M $Ni(SO_4)_2$ aqueous electrolyte (pH = 3.5) obtained from a FLUKA product. The working electrode or stationary deposition substrate as well as the counter electrode are both made of a 0.5 cm^2 area platinum plates (Goodfellow SARL Company) while a METTLER TOLEDO saturated Calomel one serves as reference for potential measurements. The electrochemical system is completed by a radiometer PGP 201 potentiostat. The film deposition method is based on the drawing of cathodic hemi-cycle current-voltage (I-V) curves within a fixed potential interval [0.00; -1.00] V/SCE, the main variable of the process being the scan rate (r) taken in the range $0.17 \leq r \leq 1.67$ $mV.s^{-1}$ usually considered as low values. A regular change of r in that selected range leads to the formation of samples having different thickness values measured from a SRATAGEM (SAMx, France) software associated with X-ray microanalysis, as reported elsewhere [11, 12]. The values obtained are corroborated by those provided by the sample cross-section images resulting from scanning electron microscopy (SEM). Global film's magnetic properties are investigated by means of a LAKE SHORE COMPANY vibrating sample magnetometer (VSM). A Nanoscope IIa (VEECO) scanning probe microscope (SPM) set operating in dual-modes serves for examination of local film's characteristics. It is then

tuned as atomic force microscope (AFM) for the film topography analyses and as a magnetic force microscope (MFM) for capturing the sample's magnetic phase images from which their magnetic microstructures are measured. The general principle of the SPM experiments in both modes is based on the determining role of the tip-sample surface interaction. Magnetic CoCr-coated tips of approximately 17 nm apex radius are connected to a cantilever of 6 Nm^{-1} spring coeficient. The system is used with a resonance frequency of about 70 Hz. SPM analyses are performed in the tapping/lift mode which allows the collection of both the topography and magnetic phase images of the same surface area. Further details on the use of each one of the applied modes are provided elsewhere [13].

3. RESULTS AND DISCUSSION

The impact of deposition substrate on material thin film's properties is well established by now even though it still remains a complex but open research topic due to interference of many other parameters [14-19]. We showed elsewhere that gold, Cu and ITO substrates respectively engender typical mechanical and microstructure features to our Ni electrodeposits whilst their fcc unit lattice remains unchanged [13, 20, 21]. Their measured strain and surface morphology including the grain's shape and size are specific in each case. One knows how these characteristics affect the film's magnetic properties. Pt substrate used in the present work keeps the same Ni film unit lattice and is then expected to bring its specific impact on the sample's microstructure and magnetic features. In the present section, the study is focused on the particular relationship between thickness (d) and root mean square surface roughness (σ) of these Ni samples [22–24]. Only the saturated roughness value precisely defined elsewhere is retained here since it is more representative of the entire sample surface irregularities [25, 26]. Implication of that relationship on the films coercivity (H_c) and magnetic domain size (w) is examined. These two film magnetic properties are chosen due to the simplicity of their well known analytical dependence on d and also because they are involved here in investigation on the Ni samples' magnetic microstructures. However, *prior to* the results presentation, an overview of our original approach to the film's characteristics seems prerequisite.

3.1. Characteristics of real mesoscopic scale thick films in a series

Evolution of a thin film property is commonly investigated from a sample's series made of specimens obtained following a precise protocol. Bringing some change to their deposition conditions is the only way to produce different specimens neatly sorted out by means of a precise discrimination criterion. This objective is reached by acting on the film deposition parameters (x_1, x_2 ..... x_n) including deposition time, t. A change in one of the selected $x_i \neq t$, keeping fixed all the other parameters, directly affects the growth rate of the film formation. That gives rise to a series of specimens having their individual (d_i, σ_i) couples. A similar result is also obtained by solely changing t value although the origin of modification in (d_i, σ_i) couples differs since the film growth rate is maintained here. In both cases, the selected x_i simultaneously affects d and σ of the specimens. Accordingly, $d_1 \neq d_2 \neq d_3 \ldots \neq d_n$ and also $\sigma_1 \neq \sigma_2 \neq \sigma_3 \ldots \neq \sigma_n$. It can be deduced that neither d nor σ is separately controlled by any x_i parameter. Besides, if evolution of d can be theoretically predicted like in electrodeposition (i.e. Faraday law), anticipating the one of σ remains very difficult. One concludes that sorting out specimens of a series only by means of their thickness d value is impossible since their surface roughness σ differs. Similarly, taking exclusively roughness criterion σ for the same operation is equally unacceptable due to the variation of their d value. When the condition $\sigma <<< d$ (with $d/\sigma \geq 10^2$) widely admitted for macroscopic scale thick samples is fulfilled, d is their only one main contributing geometrical characteristic. The sorting out operation is then executed referring to d, as commonly encountered. Under the effect of a constant physical field (E), the dependence of the resulting film property (p) on d is then nearly similar to the one of ideally flat films ($d \neq 0$, $\sigma = 0$) such as

$$p \approx \mathrm{f}(d) \qquad (1).$$

In principle, the condition ($d/\sigma \geq 10^2$) as proposed is always expected to be possibly fulfilled, regardless of the film thickness category. In actual fact, only specific growth modes can lead to its achievement with concrete microscopic scale thick samples [27, 28]. This achievement becomes very problematic for real mesoscopic scale thick samples, including nanoscopic scale thick ones and nano-structured specimens that exhibit a lower chance to directly satisfy that condition. The literature on the last sample's category seldom discusses on experimental results concurring with the condition $d/\sigma < 10^2$, which depicts impossible approximation between σ and d [29–33]. In that precise case, the extremely reduced d measurements combined with unavoidable σ values requires considering the sample's global geometrical

feature with both characteristics in term of ($d \neq 0$, $\sigma \neq 0$) couple, as mentioned above. Accordingly, each one of them has to be simultaneously considered for a consistent sample's sorting out operation. This particular situation is practically denied or eluded in the studies of material thin films. A solution can be found for that operation by using the sample non dimensional thickness to surface roughness ratio, simply named by sample geometrical ratio τ_i, expressed as

$$\tau_i = (d_i / \sigma_i) = (d / \sigma)_i \qquad (2).$$

In that precise case, τ_i appears a relevant and well adapted characteristic of each real material thin film. In the series, this ratio enables a safe sample's sorting out operation, keeping or not the initial ordering. Ultimately, τ can serve as the only one coherent variable of p corresponding to the following single function

$$p = \mathrm{f}(\tau) \qquad (3).$$

A comparison of individual sample p_i values can be safely done here, which permits a study of p evolution in an interval of τ values. As long as σ can never be higher than d, our approach unambiguously demonstrates that only two options correlating d and σ can lead to a sorting out operation in a series of real thin films. The first one, mostly adapted to mesoscopic scale thick samples, uses τ as demonstrated here; the second option, more common to macroscopic and microscopic scale thick samples, uses d. It can thus be deduced that d is an extension of τ in that operation.

By and large, sophisticate developments are praised for interpreting the evolution of thin film properties. We here show that the basic role of film geometrical feature is wrongly neglected most of the time due to some quick approximations. As reported, the impact of τ may markedly affect a sample p value whenever condition $d/\sigma < 10^2$ is validated, which is not concretely as rare as it seems to be with real mesoscopic scale thick films [29–33]. This impact reflects the material feed-back under a physical field (E) effect and then it directly contributes to the film experimental data. Consequently, the replacement of d by τ in analytical expressions of p, when required, should lead to a better closeness between calculated and measured p values.

3.2. Topography and thickness of investigated Ni samples

The visible impact of Pt substrate on Ni film's microstructure feature is provided by the surface topography images of **Fig. 1** corresponding to the samples having the two extreme d and τ values, as ordered in Table 1. In both cases, the result obtained quite differs from the needle-like grains or local conglomerates respectively engendered by Cu and ITO substrates shown elsewhere [13]. The grains repartition is here more regular, their size being almost uniform and their global shape almost preserved all over the entire film surface. The reported sample's topography images allow a rapid examination of the grain size evolution. Indeed, one notes in Fig. 1(b) that image magnification is performed for the smoothest sample (σ = 10 nm) in order to enhance the visibility of the sample surface morphology. This operation appears here necessary to satisfactorily compare it's microstructure with the one of the most disturbed surface (σ = 85 nm) of Fig. 1(a). *A priori,* this fact suggests that the evolution of grain size or surface irregularities is significantly quicker with Pt substrate.

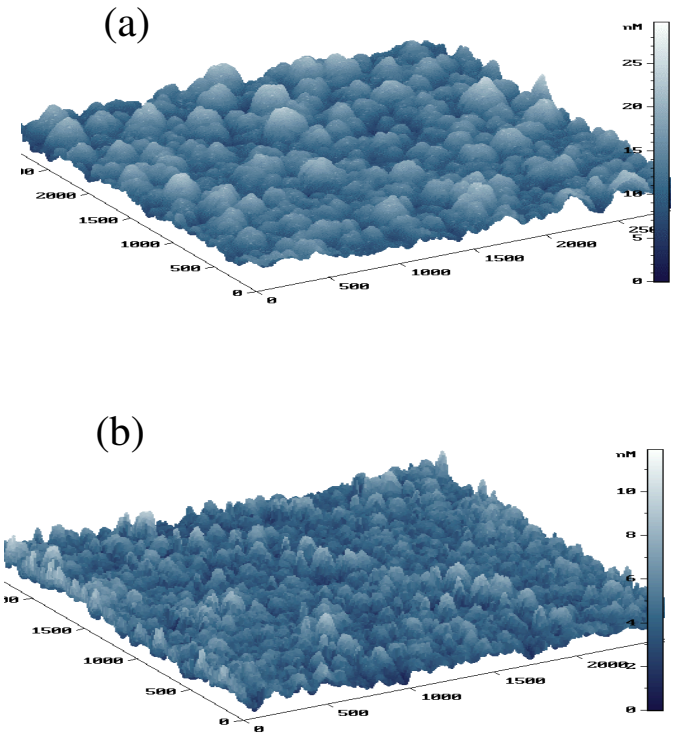

Figure 1. – 3D-AFM surface topography images of the two Ni samples having the extreme characteristics as shown in Table 1): a) – Sample 1 (with d = 102 nm and σ = 85 nm); b) – Sample 6 (with d = 820 nm and σ = 10 nm).

The results reported in Table 1 have some common features with those observed earlier with the other mentioned substrates, which are mainly assigned to the film deposition technique involved. Although the thickness limits always differ with the substrate used, the values obtained here are located in the interval $102 \leq d \leq 820$ nm, which is typical of mesoscopic scale thick samples (d <1 μm). Their measured surface roughness values are ranged in the region $10 \leq \sigma \leq 85$ nm. As depicted in **Fig. 2**, thinner samples have the higher roughness values and *vice versa* in agreement with previous experimental observations [13]. We already explained that evolution by the determining role of scan rate in the dynamics of the film deposition process, which confirms the relevancy of (C–V) technique used for elaboration of smoother thick samples. The behavior of sample geometrical ratio τ versus d reported in the same figure provides a new feature of the film characteristic's modification. Although τ regularly follows the increase of d, its evolution exhibits two different regimes in the investigated d values. The first one corresponds to a moderate increase of that ratio below $d \approx$ 530 nm while the second step depicts a tremendous enhancement of its value beyond that sample thickness. As shown in Table 1, the thinnest sample leads to $\tau = 1.23$, which evidences the fact that σ cannot be neglected compared to d. The ratio $\tau = 82.00$ of the thicker sample implies that approximation $\sigma <<< d$ is not yet acceptable although that condition is about to be fulfilled, knowing that $\tau = 100$ represents our accepted minimal limit of negligibility. One deduces from the obtained ratio evolution that the individual role of d and σ is never identical for all the Ni samples of the series. The range of the reported τ values implies that σ can never be neglected compared to d for all our investigated samples. This result clearly justifies the use of our approach of sub-section 3.1 and leads to neatly sort out the Ni samples of the series as proposed in Table 1 referring to τ, their only one common characteristic.

d (nm)	102	127	160	320	530	820
σ (nm)	85	72	56	43	25	10
$\tau = (d/\sigma)$	1.23	1.76	2.85	7.44	21.22	82.00
Samples order	1	2	3	4	5	6

Table 1 – Thickness, roughness and ordering of the investigated Ni samples sorted out by their geometrical ratio characteristic (τ).

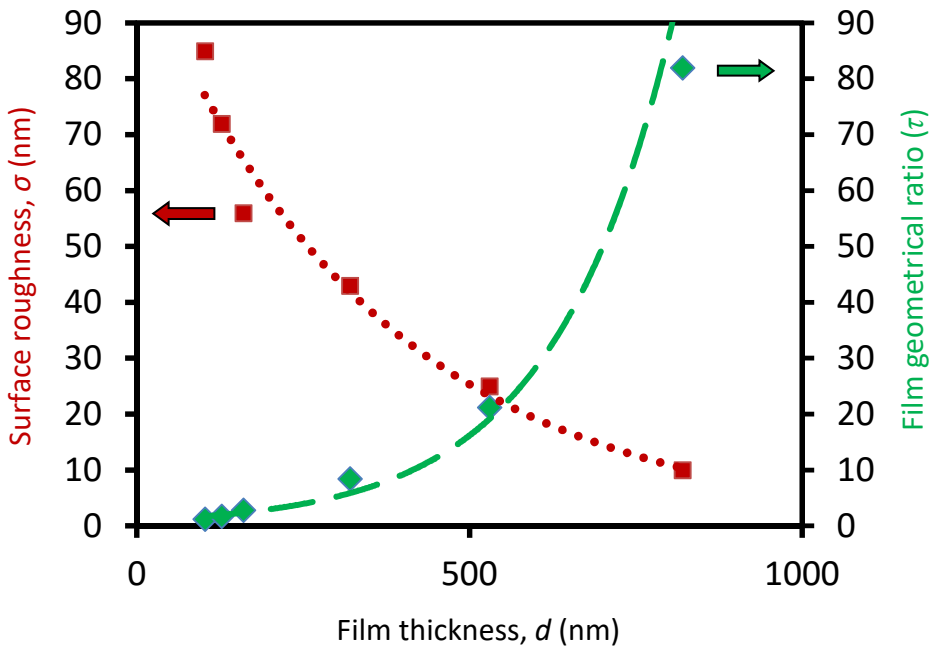

Figure 2. – Dependence of sample surface roughness (σ) and geometrical ratio (τ) on the investigated Ni film thickness value (d).

3.3. Study of global and local magnetic characteristics of Ni samples

The significance of the ratio interval $1.23 \leq \tau \leq 82.00$ reported above confirms the fact that the properties of the investigated Ni samples are more correctly studied from the approach expressed by equation (3). In that case, τ affects all their global magnetic properties including the saturation magnetization (M_s), remanence (M_r) and coercivity (H_c). The role of τ is clearly depicted in **Fig. 3** from the effect of a parallel magnetization M ($H_{\parallel}$) of the two samples numbered 1 (τ = 1.23) and 6 (τ = 82.00) in the applied field region $-1 \leq H_{\parallel} \leq +1$ KOe. The resulting hysteresis loop of the sample corresponding to the higher ratio τ = 82.00 is more tilt than the one associated with τ = 1.23. This fact suggests the occurrence of some change in the Ni sample's global magnetic properties within the region $1.23 \leq \tau \leq 82.00$.

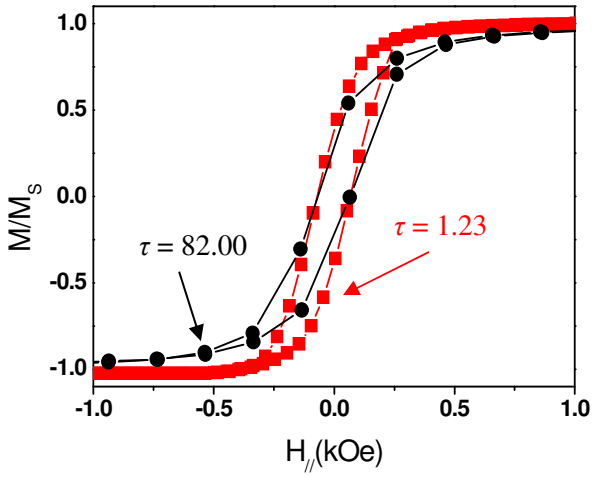

Figure 3. – Normalized magnetization (M/Ms) versus applied parallel magnetic field ($H_{\parallel}$): hysteresis loops of the two Ni samples having the extreme geometrical ratio values (τ = 1.23 and 82.00).

A confirmation of change is provided in **Fig. 4** by the study of film's coercivity and magnetic squareness $S = (M_r/M_s)$. The impact of the film geometrical feature induced by Pt substrate on the behaviour of each magnetic property is here evidenced. One sees in Fig. 4(a) that all the obtained S values are superior to 0.50. This experimental $S = f(\tau)$ curve profile can be directly and exclusively compared only with those of similar mesoscopic scale thick samples for which τ characteristic is also established. However, as long as d is considered as an extension of τ for the same material thin film taken from macroscopic till mesoscopic scale thick forms, the evolution of S versus τ or d has the same physical interpretation. One knows that higher squareness values ($S > 0.50$) of ferromagnetic films indicate that the sample's magnetic reversal is ruled by *DW* nucleation and motion mechanism [34, 35]. Consequently, the $S = f(\tau)$ curve profile of Fig. 4(a) has the same meaning. The dependence of film's coercivity H_c on τ in Fig. 4(b) depicts a regular decreasing profile which experimentally corresponds to the exponent law

$$H_c = 85.11\ (\tau)^{-0.12} \qquad (4).$$

As it appears, that curve profile concurs quite well with Néel prediction law $H_c = A\ d^{-n}$ (with A and n, the fitting constants) assigned to ferromagnetic films for which coercivity proceeds from *DW* motion mechanism [36], as found here. Owing to the close link established above between τ and d, one deduces that experimental $H_c = f(\tau)$ curve of Eq. 4 describes the same physical property behaviour .

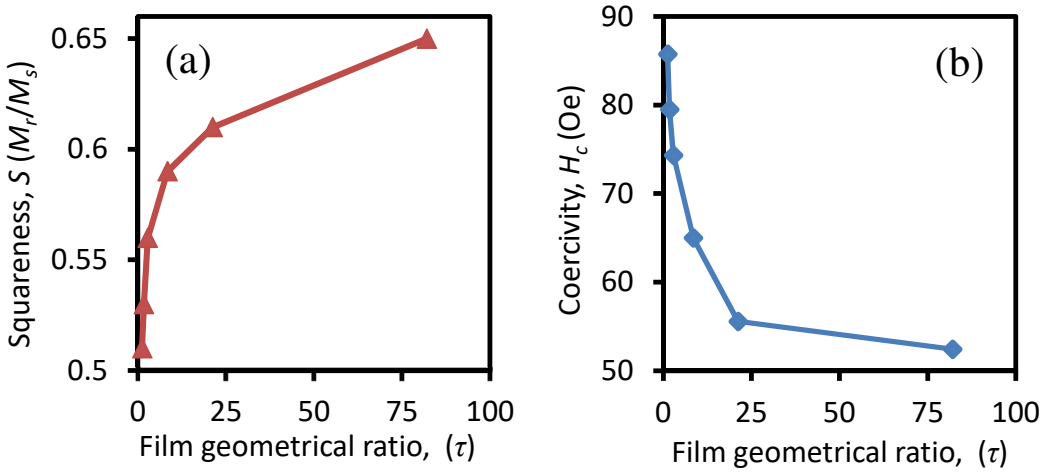

Figure 4. – Dependence of the global magnetic properties of Ni samples on their geometrical ratio: a) – Evolution of magnetic squareness (S=M_r/M_s); b) – Evolution of film's coercivity (H_c).

The local topography and magnetic imaging studies of the two samples corresponding to τ = 1.23 (labelled I) and 82.00 (labelled II) are proposed in **Fig. 5**. Strictly the same locale surface zones are examined by AFM and MFM for each one of them. Their individual SPM images, topography and magnetic line profiles are equally drawn from the same surface. One sees with each of the samples that topography images of Figs. 5(*a*) and (*c*) quite differs from those of their magnetic phase ones of Figs. 5(*b*) and (*d*). The bright and dark dots of each image type have specific meanings. In the topography images, they reflect the sample's grain height or size features. The bigger grains of the sample labelled τ = 1.23 (I) provide the higher and larger profile signals along the selected line as shown in Fig. 5(*a*). This somehow contrasts with the smaller profile signals of Fig. 5(*c*) linked to the sample labelled τ = 82.00 (II). Note that these topography profiles concur quite well with the film surface features proposed in Fig. 1. The bright and dark dots of magnetic phase images rather represent the electron spin states which respectively correspond to the repulsive (up) and attractive (down) interactions. The results proposed in Figs. 5(*b*) and (*d*) clearly reveal that the magnetic phase images and the related profile signals of the two samples are specific and do not systematically reproduce their topography configurations. The two magnetic phase images depict a variety of interconnected serpentine patterns consisted of magnetic domains (*MD*) and domain walls (*DW*) of different sizes. Their presence suggests that the investigated Ni films always have a predominant in-plane magnetic anisotropy along with a little component of out-of-plane one, as explained elsewhere [37, 38].

(a)

All the investigated sample magnetic phase images served for the determination the film magnetic domain size (w) using the measurement method proposed by Hsieh *et al* [39] and also Dumas-Bouchiat *et al* [37].

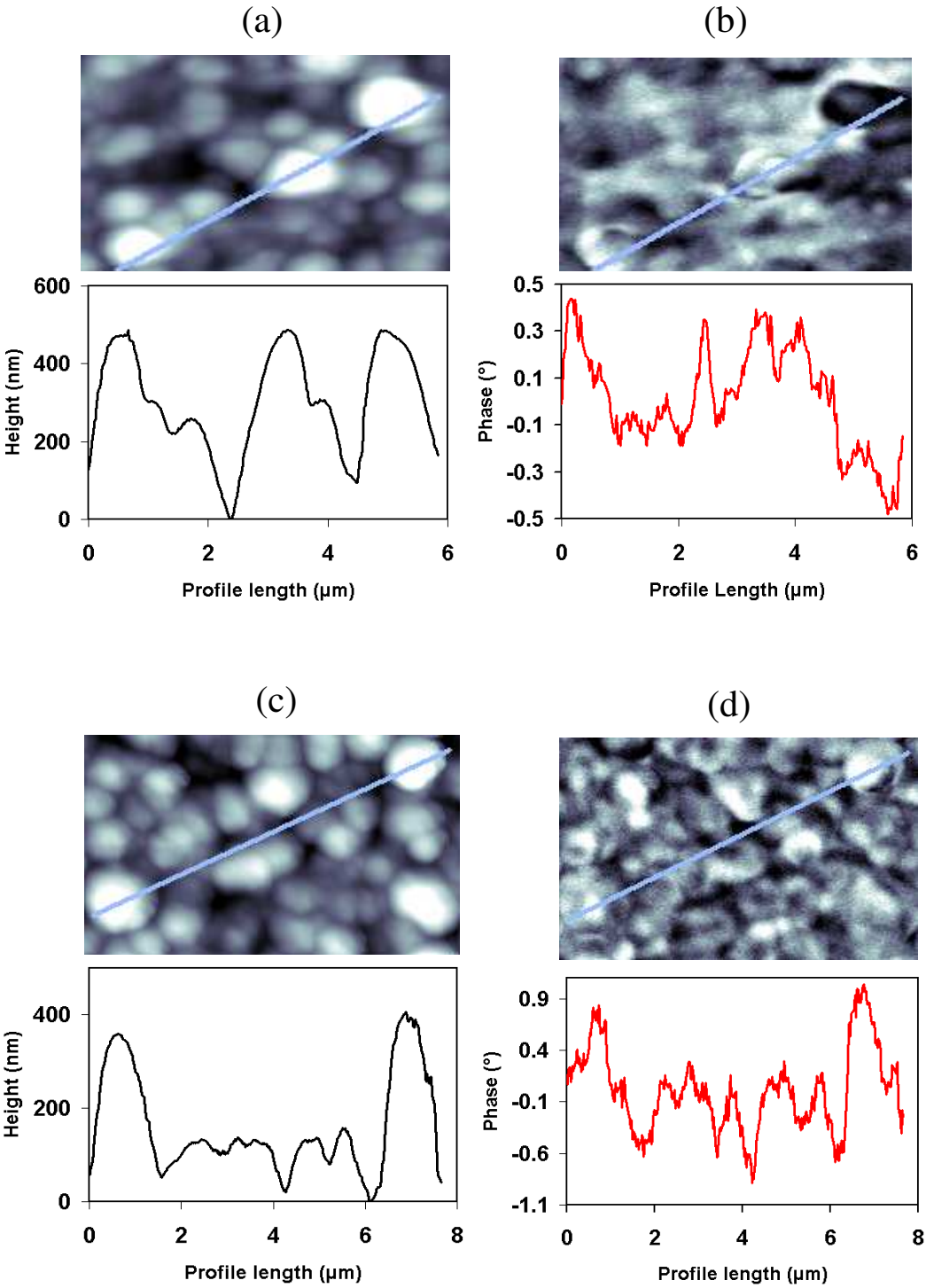

Figure 5. – Local SPM analyses of Ni samples related to the two extreme geometrical ratio values: (I) – (a) topography image and profile; (b) magnetic phase image and profile for the sample labeled τ = 1.23. (II) – (c) topography image and profile; (d) magnetic phase image and profile for the sample labeled τ = 82.00.

It should be pointed out that the dependence of w on d expressed as $w = K\ (d^{1/2})$, with K the direct proportionality constant, has been proposed by Kittel for ferromagnetic films whose coercivity has the *DW* motion origin [39, 40]. In agreement with the relationship suggested above between d and τ, we here test the real w dependence of Ni samples with respect to $(\tau^{1/2})$, without any modification of Ni/Pt system.

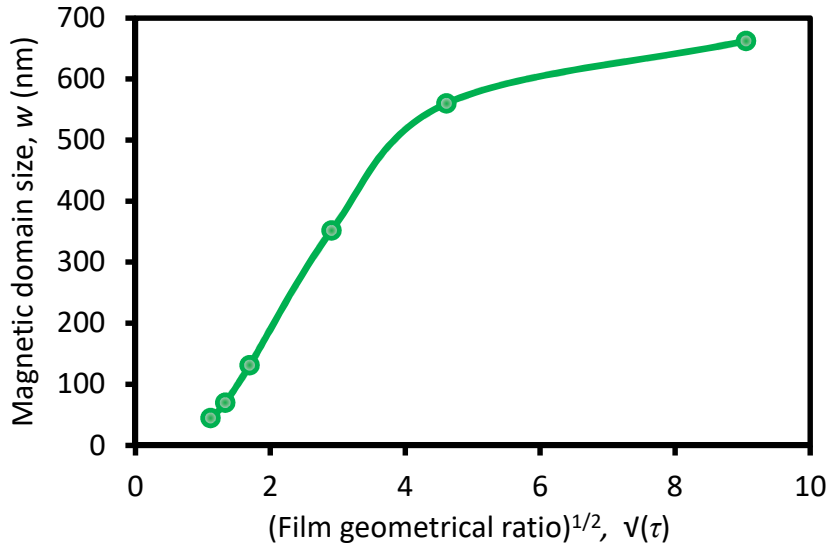

Figure 6. – Dependence of the investigated Ni samples magnetic domain size (w) on their geometrical ratio (τ).

The corresponding curve proposed in **Fig. 6** clearly shows a dependence obeying the law

$$w = 147\ \mathrm{f}\ (\tau^{1/2}) \qquad (5)$$

with K=147, whose profile is quite similar to the one expected from the mentioned Kittel w = f(d) prediction. Indeed, the straight line feature obtained for the large beginning part of this curve depicts a proportionality previously reported in the study of the $w = \mathrm{f}\ (d^{1/2})$ curve profile of Ni and Co samples [36]. One deduces from the present result that the use of d or τ keeps unchanged the linear dependence of w magnetic property, which confirms the common role played by each one of these two film geometrical characteristics. The deviation from the straight line zone reported at $(\tau^{1/2}) \approx 4.60$ has been also observed with $w = \mathrm{f}\ (d^{1/2})$ curves and assigned to some changes in the sample's magnetic patterns [34]. The same phenomenon is then likely to be the origin of the mentioned modification.

3.4. Magnetic microstructures evolved in Ni nanostructured films

The behavior of ferromagnetic sample's global and local magnetic characteristics is determined by their magnetic microstructure's types. As observed above from the studies of Ni samples surface morphology and magnetic properties, Pt deposition substrate is expected also to impact the Ni sample's magnetic microstructures. By and large, their types are examined from the film magnetic properties for which thickness has a prominent role. The influence of roughness in that matter got a late attention while the combined contribution of thickness and roughness, as proposed in the present work, still remains poorly investigated. Regarding our particular mesoscopic scale thick Ni sample's category, the study requires considering the dependence of their magnetic properties on τ, as shown above. This study is here deduced from the well adapted analytical treatment devoted to relative or normalized characteristics of ferromagnetic samples detailed elsewhere [11]. This treatment is based on the behavior of the film's normalized magnetic properties, referring to unit film thickness *versus* normalized film roughness ($\sigma' = \sigma/d$), which corresponds to reciprocal non dimensional geometrical ratio (τ^{-1}) of the present approach. Magnetic microstructure types are then directly correlated to evolution of normalized coercivity (H_c') and magnetic domain size (w'). In that case, the re-written film normalized magnetic domain size ($w'=w/d$) corresponds to

$$w' = \left[\frac{2\,E_{DW}\,(\tau)}{K_1 + \pi\,N\,{M_S}^2}\right]^{1/2} \qquad (6)$$

where E_{DW} represents the domain wall (DW) surface energy; N, the demagnetizing factor; K_1, the in-plane anisotropy constant and M_s, the saturation magnetization. Due to DW nucleation and motion mechanism of the investigated Ni samples, their normalized coercivity ($H_c' = H_c/d$) is expressed as

$${H_c}' = \frac{1}{2M_S}\left[\frac{A\,\pi^2}{\delta'} + \frac{K_v\,\delta'}{2} + \frac{\delta' + 2\,{\delta'}^2}{(1+\delta')^2}\,\pi\,{M_S}^2\right]\tau^{-1} \qquad (7)$$

with δ' the normalized DW thickness, K_v and A being respectively the in-plane volume anisotropy and the exchange constants.

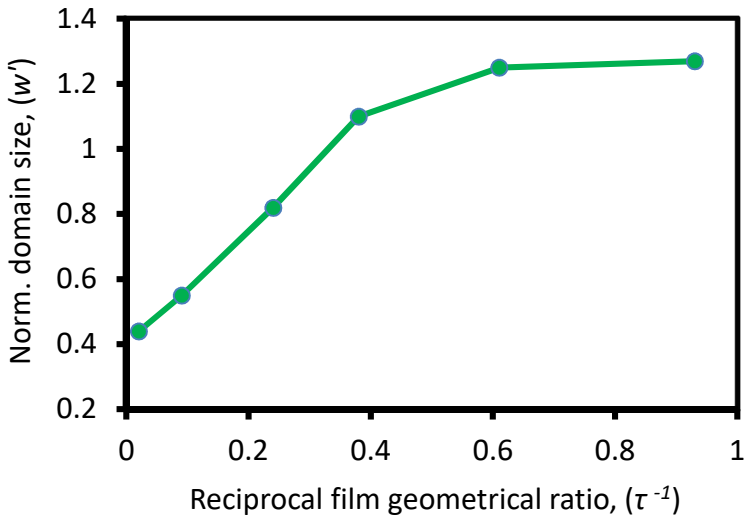

Figure 7. – Dependence of the normalized magnetic domain size (w') of the investigated Ni samples on their reciprocal geometrical ratio (τ^{-1}).

The reported experimental result of **figure 7** shows that the samples w'= f (τ^{-1}) curve profile exhibits two different regimes depending on (τ^{-1}) region. A regular increase of w' is observed below (τ_0^{-1}) ≈ 0.35, which is followed by a stabilization onset located beyond that value. The study of the samples H_c' versus (τ^{-1}) proposed in **figure 8** depicts an opposite curve profile since a moderate increasing regime of H_c' value precedes an abrupt enhancement of that property occurred also at (τ_0^{-1}) ≈ 0.35 or τ_0 ≈ 2.86. One deduces from both resulting curve profiles that different magnetic microstructure types evolved both side hands of $(\tau^{-1})_0$ value.

In the frame of the analytical treatment considered, evolution of (w') or (H_c') with respect to (τ^{-1}) provides a signature of the active magnetic microstructure type. The abrupt increasing trend of w' obtained below (τ_0^{-1}) in Fig. 7 is interpreted as the contribution of Bloch magnetic domain $(MD)_B$. The increasing trend of H_c' is rather assigned to the Néel domain walls $(DW)_N$ activity. The moderate increasing regime of this property at the same (τ_0^{-1}) region reported in Fig. 8, can thus be consistently explained by the simultaneous contributions of $(DW)_N$ and Bloch domain walls $(DW)_B$, the last type being gradually replaced by the first one. According to the same treatment, the marked increase of w' versus (τ^{-1}) is a signature of active $(MD)_B$ while its decrease is associated with Néel magnetic domain $(MD)_N$. Consequently, the moderate increase of w'= f (τ^{-1}) curve profile towards a plateau as obtained beyond $(\tau^{-1})_0$ in Fig. 7 can be assigned to the presence of both magnetic domain types. The reported stabilization onset of w' in the same figure hence corresponds to an attenuation of $(MD)_B$ activity which is gradually replaced by an enhanced role of $(MD)_N$ type. The marked increase

of H_c' in the same (τ^{-1}) region, as shown in Fig 8, can then be exclusively ascribed to the only one role of $(DW)_N$ type.

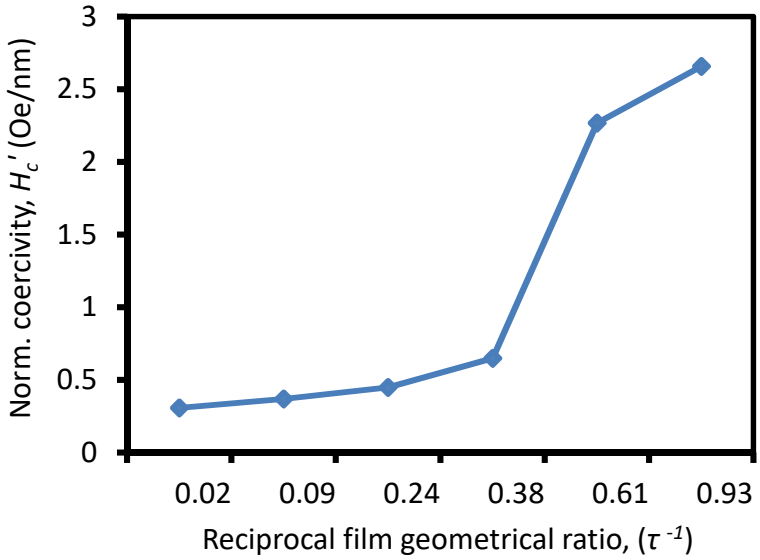

Figure 8. – Dependence of the normalized coercivity (H_c') of the investigated Ni samples on their reciprocal geometrical ratio (τ^{-1}).

4. SUMMARIZE AND CONCLUSION

Due to the unavoidable interconnection of thickness d and roughness σ resulting from thin film growth process, the study of nano-structured samples' magnetic properties is problematic when condition $(d/\sigma)<10^2$ is fully validated. Defining a new film non dimensional geometrical ratio $\tau = (d/\sigma)$ is prerequisite in that case in order to sort out the specimens of a sample's series. That ratio safely serves as a consistent variable for the study of these properties which can be expressed in a general single function form $p = f(\tau)$. That new approach is experimented here for studying coercivity (H_c) and magnetic domain size (w) of Ni electrodeposits for which the condition $(d/\sigma) <10^2$ is clearly fulfilled. When τ substitutes d, the results obtained with both properties are in agreement with theoretical predictions, implying that τ is equivalent to d and then well-adapted to the real geometry of investigated samples. Updated normalized treatment applied to these Ni films shows a discontinuity in the magnetism of these samples at $\tau_0 \approx 2.86$. Below (τ_0^{-1}), Bloch magnetic domains $(MD)_B$ coexist with mixed domain walls ($DW_N + DW_B$) while Néel domain walls $(DW)_N$ are associated with mixed magnetic domains ($MD_B + MD_N$) beyond that critical value. This preliminary contribution unambiguously reveals that τ concurs quite well with the study of

ferromagnetic samples for which approximation between d and σ is impossible. An appropriate use of τ in theoretical analyses is expected leading to more accurate results in better closeness with experimental data. In the light of the present approach, examination of different ferromagnetic material thin films remains the main concern of next investigation steps aims at confirming the real practical interest of the present proposal.

References

[1] J. F. Chang, H. H. Kuo, J. C. Leu, M. H. Hon, *Sciences and Actuators* **B 84** (2002) 258

[2] H. C. Kim, D. R. Allee, *Appl. Phys. Lett.* **81** (2002) 4287

[3] Y. Zhang, C. Tay-Rong, B. Zhou, C. Yong-Tao, H. Yan, Z. Liu, F. Schmitt, J. Lee, R. Moore, Y. Chen, H. Lin, H.-T. Jeng, S.-K. Mo, Z. Hussain, A. Bansil, Z.-X. Shen, *Nat. Nanotechnol.* **9** (2014) 111

[4] J. Barnas, Y. Bruynseraede, *Europhys. Lett.* **32** (1995) 167

[5] G. Fishman, D. Calecki, *Phys. Rev. Lett.***, 62** (1989) 1302

[6] K. A. Delin, A. W. Kleinsasser, *Supercond. Sci. Technol.* **9** (1996) 227

[7] L. Nzoghe-Mendome, J. Ebothé, M. Molinari, *J. Appl. Phys.* **109** (2011) 024904 – (1-7)

[8] Y. Arnaud, M. Brunel, A. M. De Becdelivre, P. Thevenard, *J. Chim. Pys.* **84** (1987) 341

[9] A. Barbier, G. Renaud, O. Robach, *J. Appl. Phys.* **84** (1998) 4259

[10] S. Aggarval, A. K. Goel, R. K. Mohindra, P. K. Ghosh, A. Chand, *Thin Solid Films* **223** (1993) 72

[11] J.-L. Pouchou, *Anal. Chim. Acta*, **283** (1993) 81

[12] H. Benhayoune, N. Dumelié, G, Balossier, *Thin Solid Films* **493** (2005) 113

[13] J. Ebothé, L. Nzoghe-Mendome, A. Aloufy, *Surf. Topogr.: Metrol.Prop.* **3** (2015) 045002 (10 pp)

[14] E. Gomez, A. Labarta, A. Llorente, E. Vallés, *J. Electroanal. Chem.* **2517** (2001) 63

[15] C. Rajashree, A. R. Balu, V. S. Nagarethinam, *Int. J. Chem. Techn. Res.* **6** (2014) 347

[16] H. Kachatryan, S.-N. Lee, K.-B. Kim, M. Kim, *Metals* **9**(2019); doi:10.3390/met9010012

[17] C. Mattevi, G. Eda, S. Agnoli, S. Miller, K. A. Mkhoyan, O. Celik, D. Mastrogiovanni, G. Granozzi, E. Garfunkel, M. Chhowalla, *Adv. Funct. Mater* **19** (2009) 2577

[18] H. Kim, C. M. Gilmore, A. Piqué, J. S. Horwitz, H. Mattoussi, H. Murata, Z. H. Kafali, D. B. Chrisey, *J. Appl. Phys.* **86** (1999) 6451

[19] J. C. Wittman, P. Smith, **352** *Nature* (1991) 414

[20] J. Ebothé, *Surf. Topogr.:Metrol.Prop.,* **2** (2014) 025006 (9pp)

[21] L. Nzoghe-Medome, J. Ebothé, A. Aloufy, I. V. Kityk, *J. Alloys & Compounds* **459** (2008) 232

[22] E. Hartmann, P. O. Hahn, R. J. Behm, *J. Appl. Phys.* **69** (1991) 4273

[23] J. Ebothé, *Semicond. Sci. Technol.* **11** (1996) 1096

[24] J. Krim, I. Heyvaert, C. Van Haesenconck, Y. Bruynseraede, *Phys. Rev. Lett.* **70** (1993) 57

[25] M. Hiane, J. Ebothé, *Eur. Phys. J. B* **22** (2001) 485

[26] L. Nzoghe-Mendome, A. Aloufy, J. Ebothé, D. Hui, M. El Messiry, *Mater. Chem. Phys.* **115** (2009) 551

[27] I. Petrov, P. B. Barna, L. Hultman, J. E. Greene, *J. Vac. Sci. Technol. A* **21** (2003) S117

[28] F. L. Forgerini, R. Marchiori, *Biomatter* **4** (2014) 28871

[29] Ch. Joos, A. Forkl, R. Warthmann, H.-U. Habermeier, B. Leibold, H. Kronmüller, *Physica C* **266** (1996) 235

[30] Y. Cao, C. Zhou, *J. Magn. Magn.Mater.* **333** (2013) 1

[31] D. Li, Y. Chen, Y.-W. Chung, Jr F. Lazaro Freire, *J. Vac. Sci. Technol. A* **21** (2003) L19

[32] G. Hu, G. Orkoulas, D. C. Panagiotis, *Chem. Engin. Sci.* **64** (2009) 3903

[33] M. F. Chioncel, H. S. Nagaraja, F. Rossignol, P. W. Haycock, *J. Magn Magn. Mater.* **313** (2007) 135

[34] J. Swert, K. Temst, N. Vandamme, C. Van Haesendonck, Y. Bruynseraede, *J. Magn. Magn. Mater.* **240** (2002) 380

[35] S.-M. Chérif, A. Layadi, J. Ben Youssef, C. Nacereddine, Y. Roussigné, *Physica* B **387** (2007) 281

[36] Y. Tang, D. Zhao, D. Shen, J. Zhang, B. Li, Y. Lu, X. Fan, *Thin Solid films* **516** (2008) 2094

[37] F. Dumas-Bouchiat, H.-S. Nagarja, F. Rossignol, C. Champeaux, A. Catherinot, *Appl. Surf. Sci.* **247** (2005) 76

[38] Z.-H. Wang, K. Chen, Y. Zhou, H. Zeng, *Ultramicroscopy* **105** (2005) 343

[39] C. T. Hsieh, J. Q. Liu, J. T. Lue, *Appl. Surf. Sci.* **252** (2005) 1899

[40] M. Pratzer, H. J. Elmers, M. Bode, O. Pietzch, A. Kubertzka, R. Wiesendanger, *Phys. Rev. Lett.* **87** (2001) 12701– (4p)